Density Functional Theory Calculations of the Electron Paramagnetic Resonance Parameters for VO^{2+} Complexes

Alexander C. Saladino and Sarah C. Larsen*

Department of Chemistry, University of Iowa, Iowa City, Iowa 52242

Received: October 23, 2002; In Final Form: December 30, 2002

Density functional theory calculations of electron paramagnetic resonance (EPR) parameters, such as electronic **g** tensors and metal hyperfine interaction (**A**) tensors, have been completed for a series of VO^{2+} complexes. **g** tensors were calculated with the zeroth-order regular approximation (ZORA) for relativistic effects as incorporated into the Amsterdam Density Functional (ADF) program. The **A** tensors were calculated by relativistic and nonrelativistic methods as implemented in ADF and Gaussian98 programs, respectively. The best overall agreement with experimental *A* values was obtained with the nonrelativistic method and the half-and-half hybrid functionals, such as BHPW91, BHP86, and BHLYP. The isotropic *A* values (A_{iso}) calculated nonrelativistically with the BHPW91 functional deviated by about 10% from the experimental A_{iso} values. The A_{iso} values calculated with the relativistic effects and pure generalized gradient correction (GGA) functionals, such as BP86, deviated systematically by approximately 40% compared to the experimental A_{iso} values. The difference in performance of the two methods for these complexes is attributed to the improved performance of hybrid functionals for treating core shell spin polarization. The calculation of the anisotropic or dipolar hyperfine interactions, A_D, was less sensitive to the choice of functional, and therefore, the relativistic and nonrelativistic calculations of A_D exhibited comparable accuracy.

1. Introduction

Electron paramagnetic resonance (EPR) spectroscopy is widely used to investigate the electronic environment of paramagnetic transition metals, such as vanadium(IV), in biological systems. Vanadium(IV) has a d^1 electronic configuration with one unpaired electron. The EPR parameters, such as the electronic **g** tensor and the hyperfine coupling constant or **A** tensor, depend on the coordination of the transition metal ion and on the properties of the ligands.[1−3] Ligand field theory has been used to relate electronic structure to the measured EPR parameters.

Recent advances in computational chemistry have lead to the development of new methods based on density functional theory (DFT) for electronic structure calculations of **g** and **A** tensors. Several groups have reported computational methods for calculating **g** tensors.[4−8] The relativistic method of van Lenthe has been incorporated into a commercial software package, ADF (Amsterdam Density Functional Theory 2002.01),[9−11] which uses Slater-type orbitals (STOs).[12] In the approach of van Lenthe, the spinor of the unpaired electron obtained from a DFT calculation is used to calculate the **g** tensor for a Kramer's doublet open shell molecule. Spin−orbit coupling is included variationally by use of the zero-order regular approximation (ZORA)[13−17] to the Dirac equation.[8] An analogous relativistic method for calculating **A** tensors was also developed by van Lenthe and was similarly incorporated into the ADF program.[18] Recently, the methods of van Lenthe have been applied to the calculation of EPR parameters for transition metal complexes.[19−22] Another DFT method for calculating **A** tensors has been incorporated into Gaussian software.[23] This method does not include relativistic effects or spin−orbit coupling and uses Gaussian-type orbitals (GTOs). Kaupp and co-workers have published several papers evaluating the use of Gaussian for nonrelativistic calculations of **A** tensors for transition metal systems.[24−27] Also, Barone has calculated EPR hyperfine coupling constants using these same methods incorporated in Gaussian for organic π radicals.[28,29] The theory behind EPR hyperfine coupling constant calculations can be found in many different books.[30,31]

In this study, **g** and **A** tensor calculations were completed for the series of VO^{2+} complexes shown in Figure 1 including $[VO(H_2O)_5]^{2+}$, $VO(acac)_2$, $[VO(mal)_2]^{2-}$, $[VO(ox)_2]^{2-}$, and $VO(gly)_2$. Complexes were chosen that had readily available EPR experimental data so that the accuracy of the computational methods could be assessed. The relativistic methods of van Lenthe as incorporated into the ADF program were used to calculate the **g** and **A** tensors for each of the complexes. In addition, the **A** tensors were also calculated by nonrelativistic methods as incorporated into Gaussian98. The dependence of the calculated values on the choice of exchange-correlation functionals was examined for the series of VO^{2+} complexes. A comparison of the performance of these relativistic and nonrelativistic methods for calculations of **A** tensors of VO^{2+} complexes will be made.

2. Computational Details

Geometry Optimization. Calculations of the **g** and **A** tensors were performed by use of the molecular structures from X-ray diffraction (XRD) data for $VO(acac)_2$,[32] $[VO(mal)_2]^{2-}$,[33] and $[VO(ox)_2]^{2-}$.[34] The $[VO(mal)_2]^{2-}$ crystal structure has a water molecule in the axial position, while the $[VO(ox)_2]^{2-}$ has an equatorial water molecule. Crystal structures were not available for $[VO(H_2O)_5]^{2+}$ or $VO(gly)_2$; thus geometry optimization

* Corresponding author: fax 319-335-1270; e-mail sarah-larsen@uiowa.edu.

10.1021/jp022297o CCC: $25.00
Published on Web 02/25/2003

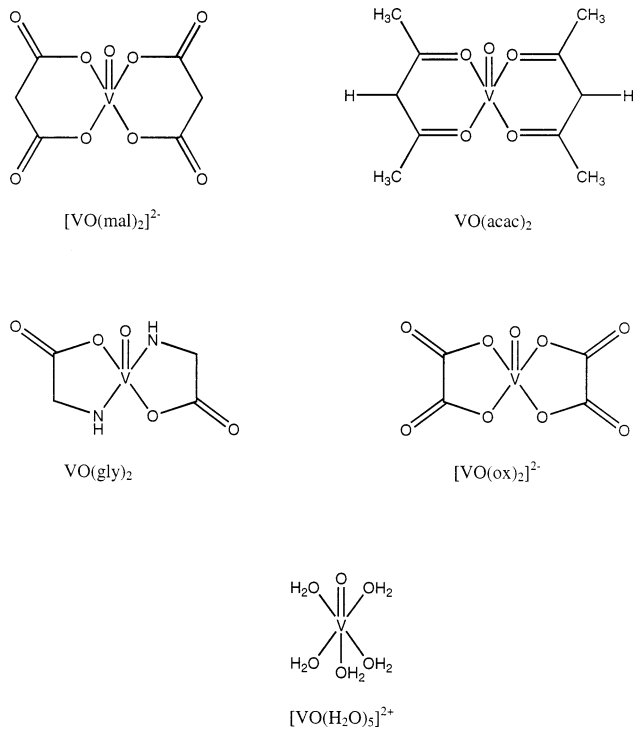

Figure 1. Vanadyl complexes studied: $[VO(mal)_2]^{2-}$, $VO(acac)_2$, $VO(gly)_2$, $[VO(ox)_2]^{2-}$, and $[VO(H_2O)_5]^{2+}$.

calculations were undertaken. The geometry optimizations were performed in Gaussian98[35] with an unrestricted Kohn−Sham calculation, TZV (triple ξ valence) basis set,[36,37] and the B3PW91 functional.[38−40] No symmetry restrictions were placed on the optimizations. Frequency calculations were performed to ensure that each optimized structure was at a minimum on the potential energy surface.

Calculations with ADF. The ADF program package (ADF 2002.01)[9−11] was used to calculate the **g** and **A** tensors for each of the VO^{2+} complexes. The methods for calculating **g** and **A** tensors were developed by van Lenthe et al.[8,18,22] and are implemented in ADF software. Two approaches can be used for **A** tensor calculations with ADF: the scalar-relativistic spin-unrestricted open shell Kohn−Sham (SR UKS) calculation and the spin−orbit coupling and scalar-relativistic spin-restricted open shell Kohn−Sham (SO + SR ROKS) calculation. In the SR UKS method, spin−orbit coupling is not included but spin polarization effects are included, making this the preferred method for calculating isotropic hyperfine coupling constants (A_{iso}). In the SO + SR ROKS method, spin−orbit coupling effects are included but not spin polarization effects. The SO + SR ROKS method is used for calculating **g** tensors and the anisotropic contribution to the hyperfine coupling constants (A_D).

Three different combinations of exchange and correlation potentials were used in the **g** and **A** tensor calculations: BLYP, BP86, and BPW91. BLYP uses the pure exchange electron gas formula as the local density approximation (LDA) with Becke gradient correction[41] for exchange and Lee−Yang−Parr correction for correlation added.[42,43] Both BP86 and BPW91 use the parametrized electron gas data given by Vosko et al. for the LDA[44] with the Becke gradient correction for exchange. BP86 uses the correlation correction by Perdew,[45] while BPW91 used the correlation correction by Perdew−Wang.[39,40,46] The basis set TZ2P was used for all calculations and all atoms.[47−50] The basis set TZ2P is a double ζ Slater-type orbital (STO) in the core and tripe ζ in the valence shell with two polarization functions.

Calculations with Gaussian98. All-electron unrestricted Kohn−Sham calculations of hyperfine tensors were conducted with Gaussian98 A11.3.[23] Relativistic effects and spin−orbit contributions were not included in the Gaussian98 calculations. However, Gaussian98 provides a much wider choice of exchange and correlation functionals and basis sets than ADF. Nine different density functionals were used in the Gaussian98 calculations; BLYP, B3LYP, BHLYP, BP86, B3HP86, BHP86, BPW91, B3PW91, and BHPW91. The first three functionals are a combination of the LYP[42,43] correlation functional with the Becke (B),[41] the Becke three-parameter (B3),[38] and the Becke half-and-half (BH)[51] exchange functionals. The next three functionals are a combination of the P86[45] correlation functional with the B, B3, and BH exchange functionals, respectively. The last three functionals are a combination of the PW91[39,40,46] correlation functional with the B, B3, and BH exchange functionals, respectively. A 15s11p6d/ 9s7p4d basis set from Kaupp et al. was used, which is a DZ (double ζ) basis set[36] with the most diffuse function of Dolg added (1s,2p,1d).[26] The SCF convergence criterion was set to 10^{-6} in RMS DM and 10^{-4} in MAX DM.

Comparison with Experimental EPR Parameters. VO^{2+} complexes with readily available experimental EPR data were chosen for this study in order to facilitate a comparison of calculated and experimental EPR parameters. Despite the careful choice of model systems, there are some issues related to the direct comparison of calculated and experimental EPR parameters that should be addressed. The experimental EPR parameters for the VO^{2+} complexes were obtained from solid-state EPR spectroscopy.[52−54] Therefore, only the absolute values of the *A* values can be determined experimentally. To facilitate a comparison with the calculated *A* values, the signs of experimental *A* values were chosen such that agreement with the signs of the calculated *A* values was maintained. Since the environment of the complex will influence the *A* values and the calculations are for gas-phase systems, better than 10−15% agreement with experimental *A* values is not expected.[26] Further research in which the effect of the environment is included in DFT calculations by use of a solvent model or other methods will be important in the future when the best computational methods for calculating *g* and *A* values for transition metals are better understood and more widely accepted. Currently, errors due to the environment are probably small compared to errors inherent in the computational methods.

3. Results and Discussion

Each of the VO^{2+} complexes studied here is in a d^1 electronic configuration with one unpaired electron. The vanadium electron−nuclear hyperfine interaction is characterized by an interaction between the unpaired electron ($S = {}^1/_2$) and the vanadium nuclear spin ($I = {}^7/_2$, 99.8% natural abundance). Two interactions contribute to the hyperfine coupling tensor: an isotropic or Fermi contact interaction, A_{iso}, and an anisotropic or dipolar hyperfine interaction, A_D.[31] The isotropic hyperfine interaction, A_{iso}, is related to the spin density at the magnetic nucleus, and therefore inclusion of spin polarization effects is particularly important for accurate calculations of A_{iso}.[22,25] In some cases, spin polarization may also have a nonnegligible effect on A_D.[25−27,55]

Relativistic Calculations of g Tensors for VO^{2+} Complexes. The **g** and **A** tensors of VO^{2+} complexes were calculated by the ADF program and the method of van Lenthe.[8,18] The principal values of the **g** tensor were calculated with three different functionals (BLYP, BP86, and BPW91) and are listed

TABLE 1: Relativistic (ADF) Calculated and Experimental *g* Values for VO^{2+} Complexes

		calcd			
molecule	*g* value	BLYP	BP86	BPW91	exp
$VO(gly)_2$	g_{11}	1.992	1.992	1.992	1.981[a]
	g_{22}	1.981	1.981	1.980	1.980[a]
	g_{33} ($g_{\|\|}$)	1.958	1.958	1.957	1.950[a]
$[VO(H_2O)_5]^{2+}$	g_{11}	1.980	1.980	1.979	1.978[b]
	g_{22}	1.978	1.977	1.977	1.978[b]
	g_{33} ($g_{\|\|}$)	1.925	1.923	1.923	1.933[b]
$VO(acac)_2$	g_{11}	1.980	1.977	1.975	1.985[c]
	g_{22}	1.972	1.968	1.966	1.979[c]
	g_{33} ($g_{\|\|}$)	1.938	1.931	1.928	1.945[c]
$[VO(mal)_2]^{2-}$	g_{11}	1.976	1.975	1.974	1.978[a]
	g_{22}	1.964	1.962	1.961	1.978[a]
	g_{33} ($g_{\|\|}$)	1.959	1.957	1.957	1.942[a]
$[VO(ox)_2]^{2-}$	g_{11}	1.979	1.979	1.979	1.978[a]
	g_{22}	1.971	1.971	1.971	1.978[a]
	g_{33} ($g_{\|\|}$)	1.941	1.945	1.945	1.941[a]

[a] Reference 54. [b] Reference 53. [c] Reference 52.

in Table 1. As expected for these calculations with the pure GGA functionals, the calculated *g* values are virtually invariant with respect to the choice of functional. Similarly, Kaupp and co-workers[4] and Ziegler and co-workers[5−7] reported little dependence on the functional with their methods for calculating *g* values of transition metal complexes. However, recent work by Neese[56] and Kaupp et al.[57] suggests that *g* value calculations may be improved by the use of hybrid functionals.

Relativistic Calculations of A Tensors for VO^{2+} Complexes. Two relativistic methods of calculating the **A** tensors for VO^{2+} complexes were compared: the SR UKS and SO + SR ROKS methods. For each method, the calculation was performed with three different functionals, BLYP, BP86, and BPW91. The results are listed in Table 2 and the results for $VO(gly)_2$ are graphed in Figures 2 and 3. Graphs of the results for the other complexes show the same trends and are provided as Supporting Information. The diagonally striped bars in Figures 2 and 3 represent the ADF results (SR UKS for A_{iso} and SO + SR ROKS for A_D), and the dotted bars represent the experimental values.

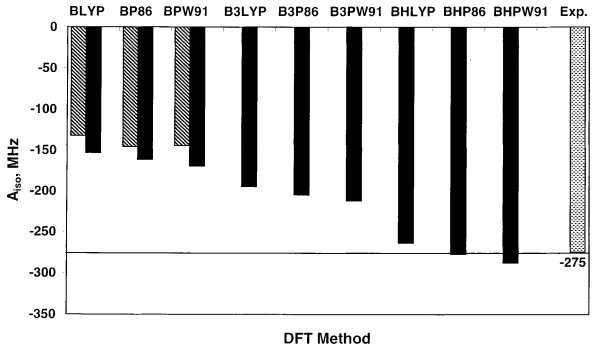

Figure 2. Comparison of calculated A_{iso} values (in megahertz) for $VO(gly)_2$ from data in Tables 2 and 3. The solid bars represent the A_{iso} values from the Gaussian98 calculations with the different functionals listed, the diagonally striped bars represent the A_{iso} values from the ADF (SR UKS) calculations with the functionals listed, and the dotted bar represents the experimentally measured A_{iso}.

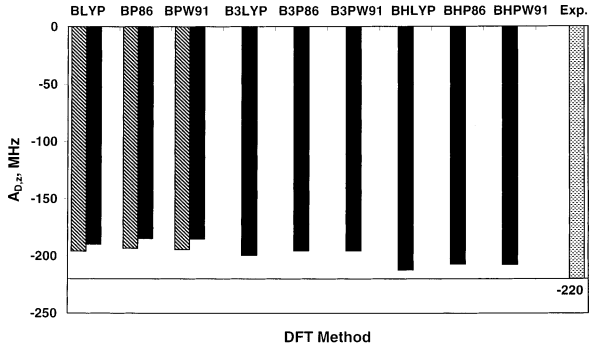

Figure 3. Comparison of calculated $A_{D,z}$ values (in megahertz) for $VO(gly)_2$ from data in Tables 2 and 4. The solid bars represent the $A_{D,z}$ values from the Gaussian98 calculations with the different functionals listed, the diagonally striped bars represent the $A_{D,z}$ values from the ADF (SO + SR ROKS) calculations with the functionals listed, and the dotted bar represents the experimentally measured $A_{D,z}$.

The A_{iso} values calculated for VO^{2+} complexes with SR UKS are approximately 50−70% of the experimental values. This is to be expected since calculations with pure GGA functionals

TABLE 2: Relativistic (ADF) Calculated and Experimental Isotropic and Dipolar Hyperfine Coupling Constants for Vanadium Model Complexes

		ADF						
		SR UKS			SO + SR ROKS			
molecule	*A* value (MHz)	BLYP	BP86	BPW91	BLYP	BP86	BPW91	exp[a]
$VO(gly)_2$	A_{iso}	−132	−145	−144	18	19	19	−275[b]
	$A_{D,x}$	100	97	97	117	117	117	115[b]
	$A_{D,y}$	78	75	76	78	77	77	105[b]
	A_{Dz}	−178	−172	−173	−196	−193	−194	−220[b]
$[VO(H_2O)_5]^{2+}$	A_{iso}	−211	−236	−234	−21	−21	−21	−324[c]
	$A_{D,x}$	92	89	90	109	109	109	112[c]
	$A_{D,y}$	93	90	90	111	110	111	112[c]
	A_{Dz}	−185	−180	−180	−220	−219	−220	−224[c]
$VO(acac)_2$	A_{iso}	−166	−186	−184	−8	−9	−10	−307[d]
	$A_{D,x}$	100	97	97	122	124	126	116[d]
	$A_{D,y}$	86	84	84	88	83	83	112[d]
	A_{Dz}	−186	−181	−181	−210	−207	−208	−228[d]
$[VO(mal)_2]^{2-}$	A_{iso}	−153	−173	−171	−3	−2	−2	−299[b]
	$A_{D,x}$	105	101	102	121	121	121	109[b]
	$A_{D,y}$	79	77	78	77	78	79	109[b]
	A_{Dz}	−184	−179	−179	−198	−199	−200	−219[b]
$[VO(ox)_2]^{2-}$	A_{iso}	−156	−175	−174	−1	−3	−3	−295[b]
	$A_{D,x}$	98	95	95	114	111	112	108[b]
	$A_{D,y}$	83	81	81	84	85	86	108[b]
	A_{Dz}	−181	−176	−176	−198	−197	−198	−217[b]

[a] A negative value for A_{iso} has been assumed for the experimental value for comparison with calculated values. [b] Reference 54. [c] Reference 53. [d] Reference 52.

TABLE 3: Nonrelativistic (Gaussian 98) Calculated and Experimental Isotropic Hyperfine Coupling Constants for Vanadium Model Complexes

		Gaussian									
molecule	*A* value (MHz)	BLYP	BP86	BPW91	B3LYP	B3P86	B3PW91	BHLYP	BHP86	BHPW91	exp[a]
$VO(gly)_2$	A_{iso}	−153	−161	−169	−194	−205	−212	−264	−277	−288	−275[b]
	$\langle S^2\rangle$[c]	0.7570	0.7579	0.7587	0.7618	0.763	0.7640	0.7757	0.7782	0.7813	0.7500
$[VO(H_2O)_5]^{2+}$	A_{iso}	−231	−246	−256	−278	−094	−304	−375	−398	−415	−324[d]
	$\langle S^2\rangle$[c]	0.7611	0.7618	0.7631	0.7741	0.7748	0.7775	0.8437	0.8476	0.8629	0.7500
$VO(acac)_2$	A_{iso}	−187	−200	−209	−224	−239	−246	−290	−308	−319	−307[e]
	$\langle S^2\rangle$[c]	0.7572	0.7579	0.7589	0.7625	0.7800	0.7648	0.7777	0.7507	0.7835	0.7500
$[VO(mal)_2]^{2-}$	A_{iso}	−170	−183	−191	−207	−221	−228	−268	−287	−297	−299[b]
	$\langle S^2\rangle$[c]	0.7574	0.7579	0.7588	0.7626	0.7636	0.7649	0.7778	0.7799	0.7831	0.7500
$[VO(ox)_2]^{2-}$	A_{iso}	−175	−188	−196	−212	−226	−233	−271	−290	−300	−295[b]
	$\langle S^2\rangle$[c]	0.7571	0.7577	0.7585	0.7621	0.7631	0.7639	0.7748	0.7769	0.7803	0.7500

[a] *A* values are given in megahertz. A negative value for A_{iso} has been assumed for the experimental value for comparison with calculated values. [b] Reference 54. [c] Before annihilation. [d] Reference 53. [e] Reference 52.

TABLE 4: Nonrelativistic (Gaussian 98) Calculated and Experimental Dipolar Hyperfine Coupling Constants for Vanadium Model Complexes

		Gaussian									
molecule	*A* value (MHz)	BLYP	BP86	BPW91	B3LY	B3P86	B3PW91	BHLYP	BHP86	BHPW91	exp
$VO(gly)_2$	$A_{D,x}$	108	106	106	111	109	109	116	114	94	115[a]
	$A_{D,y}$	82	79	79	88	86	86	96	93	114	105[a]
	A_{Dz}	−190	−185	−185	−199	−195	−196	−212	−207	−208	−220[a]
$[VO(H_2O)_5]^{2+}$	$A_{D,x}$	98	95	95	99	97	97	97	98	94	112[b]
	$A_{D,y}$	99	96	96	100	98	98	101	95	97	112[b]
	A_{Dz}	−197	−192	−192	−199	−195	−198	−198	−193	−191	−224[b]
$VO(acac)_2$	$A_{D,x}$	107	104	105	110	108	108	114	112	112	114[c]
	$A_{D,y}$	91	89	89	96	94	94	103	100	100	112[c]
	A_{Dz}	−198	−193	−193	−205	−201	−202	−217	−212	−213	−228[c]
$[VO(mal)_2]^{2-}$	$A_{D,x}$	112	110	110	115	113	113	118	115	115	109[a]
	$A_{D,y}$	83	81	81	89	87	87	96	94	94	109[a]
	A_{Dz}	−195	−190	−191	−204	−200	−200	−214	−209	−209	−219[a]
$[VO(ox)_2]^{2-}$	$A_{D,x}$	105	102	102	110	107	107	114	111	111	108[a]
	$A_{D,y}$	88	85	86	93	91	91	99	96	96	108[a]
	A_{Dz}	−193	−187	−188	−202	−198	−198	−212	−207	−207	−217[a]

[a] Reference 54. [b] Reference 53. [c] Reference 52.

have been shown to underestimate the spin polarization of the s-type metal core orbitals.[26,27] The A_{iso} values calculated for VO^{2+} complexes by the SO + SR ROKS method severely underestimate A_{iso} due to the total exclusion of spin polarization effects in this calculation. Therefore, the SR UKS method provides better A_{iso} values relative to the SO + SR ROKS method.[22,25] However, while the accuracy of the A_{iso} values calculated with the SR UKS method is still quite poor, it should be noted that the calculations systematically underestimate A_{iso} so that trends in data can be predicted by use of these methods.[58]

The A_D values calculated for VO^{2+} complexes by the SR UKS and SO + SR ROKS methods are approximately 80−90% of the experimental values, respectively. For all of the complexes considered here, the SO + SR ROKS calculations yielded the most accurate A_D values relative to the SR UKS calculations. This suggests that, for the A_D values, the spin−orbit effects are more important than the spin polarization effects. Thus, the most accurate *A* values calculated by the relativistic methods in ADF are obtained by combining A_{iso}, calculated by the SR UKS method, and A_D, calculated by the SO + SR ROKS method, as discussed recently by van Lenthe and co-workers.[22] However, this is not an ideal situation because the A_{iso} values are calculated without including spin−orbit effects and the A_D values are calculated with the inclusion of spin−orbit effects, and then these two values are combined. Just as in the case of the *g* calculations, the variation between *A* values calculated with different functionals was relatively small compared to other systematic errors inherent in the computational method. When possible, it is best to consider the two components, A_{iso} and A_D, separately.

Nonrelativistic Calculations of A Tensors for VO^{2+} Complexes. For a comparison of the relativistic methods of ADF and the nonrelativistic methods of Gaussian98, the **A** tensor for VO^{2+} complexes was also calculated with Gaussian98. Since Gaussian98 has a wider range of exchange functionals available than ADF, the dependence of the **A** tensor calculation on the functional was examined more extensively. The results are presented in Tables 3 and 4 and graphically for $VO(gly)_2$ in Figures 2 and 3. Graphs of the results for the other complexes show the same trends and are provided as Supporting Information. The solid bars in Figures 2 and 3 represent the Gaussian98 results, the diagonally striped bars represent the ADF results (SR UKS for A_{iso} and SO + SR ROKS for A_D), and the dotted bars represent the experimental results.

The A_{iso} values were calculated for VO^{2+} complexes with Gaussian98 and nine different functionals. The results for each of the VO^{2+} complexes are graphed in Figure 2 and as Supporting Information. In general, the accuracy of the A_{iso} values successively improved on going from the pure GGA functionals (BLYP, BP86, and BPW91) to the hybrid B3 functionals (B3LYP, B3P86, and B3PW91) to the half-and-half hybrid functionals (BHLYP, BHPW91, and BHP86). Generally, the most accurate results for A_{iso} were obtained when the half-and-half hybrid functionals were used. The exception to these observations is $[VO(H_2O)_5]^{2+}$. The A_{iso} values calculated with half-and-half hybrid functionals overestimated the experimental

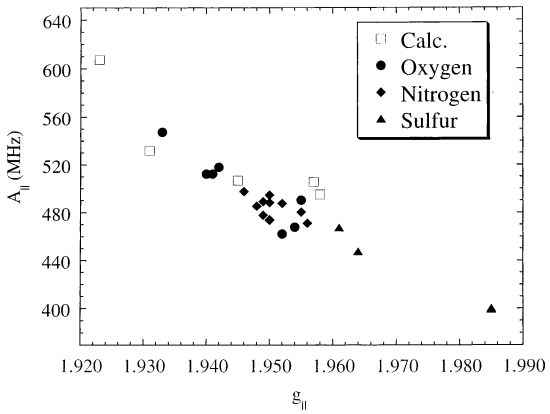

Figure 4. Graph of $g_{||}$ vs $|A_{||}|$ showing experimental EPR data from ref 41 for VO^{2+} complexes containing equatorial nitrogen (◆), oxygen (●), and sulfur (▲) ligands. Also plotted are the DFT computational results (□) for $g_{||}$ (ADF, BP86, SO + SR ROKS) and $|A_{||}|$ (Gaussian98, BHPW91) for $[VO(H_2O)5]^{2+}$, $VO(acac)_2$, $[VO(mal)_2]^{2-}$, $[VO(ox)_2]^{2-}$, and $VO(gly)_2$.

A_{iso} values for $[VO(H_2O)_5]^{2+}$, and the B3 hybrid functionals (B3LYP, B3P86, and B3PW91) provided the best numerical accuracy.

Overall, these results suggest that, for A_{iso} calculations with Gaussian98, the best agreement with experimental data is obtained with half-and-half hybrid functionals, such as BHLYP, BHPW91, and BHP86. These results are in agreement with previous studies by Munzarová and Kaupp, who observed that the A_{iso} value for transition metal complexes is dependent on the functional used in the calculation.[26] This dependence of the **A** tensor calculation on the functional has also previously been observed for organic π radicals.[28,29] For A_{iso} value calculations for vanadium(IV) with Gaussian, Munzarová and Kaupp found that the best results were obtained for the half-and-half hybrid functional, BHPW91, due to the mixing of exact exchange with the half-and-half hybrid functional, which enhances the spin polarization of s-type metal core orbitals relative to pure GGA functionals.[26] Munzarová and Kaupp also pointed out that the deficiencies in density functionals are systematic for complexes of related electronic structure,[25] which is also the case with the results presented here with the exception of $[VO(H_2O)_5]^{2+}$.

The calculations of A_D for $VO(gly)_2$ with the nonrelativistic methods of Gaussian98 are graphed in Figure 3 (solid bars). The dependence of the A_D calculations on the functional is much less dramatic than for the A_{iso} calculations. This is because the A_D values do not strongly depend on spin polarization effects. However, just as for the A_{iso} values, the half-and-half hybrid functionals generally perform best for the A_D calculations for the VO^{2+} complexes with the exception of $[VO(H_2O)_5]^{2+}$. These results are in agreement with recent work by Kaupp and coworkers on vanadyl complexes containing Schiff base ligands in which the best quantitative agreement with experimental results for A_D was obtained with the hybrid functional BHPW91.[39,40,46,51]

Comparison of Relativistic and Nonrelativistic Calculations of A Tensors for VO^{2+} Complexes. To compare the results of the **A** tensor calculations for the DFT methods discussed above, the calculated values listed in Tables 2−4 are presented graphically in Figures 2 and 3 and as Supporting Information. Inspection of Figure 2 and the solid (nonrelativistic Gaussian98) and diagonally striped bars (relativisitc ADF) for the pure GGA functionals (BLYP, BP86, and BPW91) shows that the calculated A_{iso} values are comparable for calculations with ADF and Gaussian98 when the same functional is used. In both cases, the results show that the calculations seriously underestimate the spin polarization of the s-type metal core orbitals when pure GGA functionals are used, as discussed earlier. While a direct comparison of these methods is not strictly possible because of inherent differences in the computational methods implemented in ADF and Gaussian, such as the use of STO and GTO orbitals, respectively, it seems that the accuracy is comparable when the same functional is used. In other words, when A_{iso} values are calculated for these VO^{2+} complexes, the spin polarization effects dominate all other effects. Also apparent is that, as stated previously, the best agreement with experimental data is obtained for Gaussian98 with the half-and-half hybrid functionals, such as BHLYP, BHPW91, and BHP86. For these VO^{2+} complexes, the inclusion of relativistic effects does not affect the accuracy as much as the choice of functional. Calculations of A_D were much less sensitive to the choice of functional, but the half-and-half hybrid functionals with the nonrelativistic method generally provided the best accuracy. The SO + SR ROKS relativistic method calculations of A_D with pure GGA functionals provided better accuracy compared to the nonrelativistic calculations of A_D with the same pure GGA functionals. This can be seen by considering the BLYP, BP86, and BPW91 results for A_D.

Comparison of Calculated and Experimental EPR Parameters. Despite the recent advances in computational methods, the performance of DFT calculations of EPR parameters for transition metal complexes has not been reliably quantitative. However, the deviations from experimental values are often systematic, especially for a group of related transition metal complexes. Therefore, trends in EPR parameters can be successfully reproduced and insight into the relationship between electronic structure and EPR parameters can be obtained.[19,58]

Holyk[54] previously observed that, for VO^{2+} complexes with various equatorial ligands, the parallel components of **g** and **A** were correlated as shown in Figure 4 by the solid symbols. VO^{2+} complexes with equatorial sulfur ligands (▲) have the largest $g_{||}$ values and the smallest $A_{||}$ values. VO^{2+} complexes with equatorial nitrogen (◆) and oxygen (●) ligands can be found at lower $g_{||}$ values and higher $A_{||}$ values relative to sulfur ligands, as illustrated in Figure 4. For the VO^{2+} complexes studied here, the equatorial ligands are oxygen or nitrogen. The $A_{||}$ values can be calculated from the A_{iso} and $A_{D,z}$ values listed in Tables 2−4 by use of the relationship $|A_{||}| = |A_{iso} + A_{D,z}|$. The calculated $g_{||}$ (ADF, BP86, SO + SR ROKS) and $A_{||}$ (Gaussian98, BHPW91) for the model complexes are also plotted in Figure 4 (□). The calculated values fit onto the graph and reproduce the experimentally observed trends in $g_{||}$ and $A_{||}$ rather well. It should be noted that the calculated $A_{||}$ values have not been scaled (as was necessary in our previous work[20]) due to the improved performance of the hybrid functionals relative to the pure GGA functionals for calculating **A** tensors.

In addition, the dependence of the calculated $g_{||}$ (ADF, BP86) and $A_{||}$ (Gaussian98, BHPW91) values on the V═O bond length (in angstroms) for the complexes $[VO(H_2O)_5]^{2+}$, $VO(acac)_2$, $[VO(mal)_2]^{2-}$, $[VO(ox)_2]^{2-}$, and $VO(gly)_2$ has been investigated as shown in Figure 5. V═O bond lengths from crystal structures were used for all complexes except for $[VO(H_2O)_5]^{2+}$ and $VO(gly)_2$, for which the optimized V═O bond lengths were used. The $g_{||}$ values (□) and the $A_{||}$ values (●) are represented in Figure 5. The resulting graph in Figure 5 suggests that $g_{||}$ increases with increasing V═O bond length and $A_{||}$ decreases with increasing V═O bond length. The $g_{||}$ data show much more scatter then the $A_{||}$ data. A similar trend was observed previously by us for model VO^{2+} complexes with similar geometries.[20]

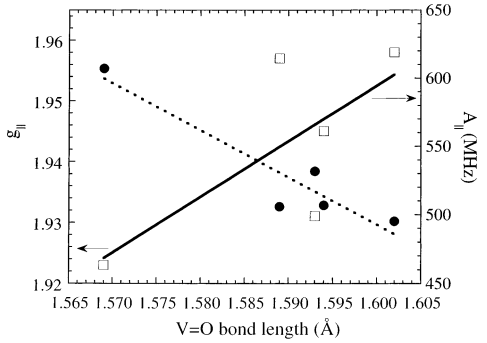

Figure 5. Dependence of the calculated $g_{||}$ (ADF, BP86, SO + SR ROKS, □) and $|A_{||}|$ (Gaussian98, BHPW91, ●) values on the VO bond length (in angstroms) for these complexes, $[VO(H_2O)_5]^{2+}$, $VO(acac)_2$, $[VO(mal)_2]^{2-}$, $[VO(ox)_2]^{2-}$, and $VO(gly)_2$. V═O bond lengths from crystal structures were used for all complexes except for $[VO(H_2O)_5]^{2+}$ and $VO(gly)_2$, for which the optimized V═O bond lengths were used.

This may be the underlying structural feature that establishes the correlation of $A_{||}$ and $g_{||}$ observed in Figure 4. However, a more comprehensive investigation of VO^{2+} complexes is needed before this correction can be definitively established.

4. Conclusions

DFT methods were utilized to calculate the EPR parameters for several VO^{2+} complexes. **g** tensors were calculated by the ADF program and **A** tensors were calculated by relativistic and nonrelativistic methods incorporated into ADF and Gaussian98 programs, respectively. Comparable accuracy was observed for the relativistic (ADF) and the nonrelativistic methods when **A** tensors for VO^{2+} complexes were calculated with the same functional (BP86, BLYP, or BPW91). However, the agreement of the A_{iso} values with experimental data was significantly improved when hybrid functionals, such as BHLYP, BHPW91, and BHP86, were used in the Gaussian98 calculations. The calculations of A_D was less sensitive to the choice of functional used in the calculation.

Acknowledgment. S.L. gratefully acknowledges the support of NSF (CHE-02048047) and the University of Iowa (Carver). A.S. acknowledges M. L. Munzarová for assistance with Gaussian98 calculations. The calculations were performed on IBM RS/6000 workstations obtained through an NSF CRIF grant (CHE-9974502) and on the supercomputer through the National Computational Science Alliance (CHE010042 and CHE020051).

Supporting Information Available: Optimized Cartesian coordinates for $[VO(H_2O)_5]^{2+}$ and $VO(gly)_2$, listed in Tables S1 and S2, respectively, and data from Tables 1−4, graphed in Figures S1−S8. This material is available free of charge via the Internet at http://pubs.acs.org.

References and Notes

(1) Chasteen, N. D. Vanadyl(IV) EPR Spin Probes: Inorganic and Biochemical Aspects. In *Biological Magnetic Resonance*; Berliner, L. J., Reuben, J., Eds.; Plenum: New York, 1981; Vol. 3, p 53.

(2) Prakash, A. M.; Kevan, L. *J. Phys. Chem. B* **2000**, *104*, 6860−6868.

(3) Peisach, J.; Blumberg, W. E. *Arch. Biochem. Biophys.* **1974**, *165*, 691−708.

(4) Malkina, O. L.; Vaara, J.; Schimmelpfennig, B.; Munzarová, M.; Malkin, V. G.; Kaupp, M. *J. Am. Chem. Soc.* **2000**, *122*, 9206−9218.

(5) Patchkovskii, S.; Ziegler, T. *J. Chem. Phys.* **1999**, *111*, 5730−5740.

(6) Patchkovskii, S.; Ziegler, T. *J. Am. Chem. Soc.* **2000**, *122*, 3506−3516.

(7) Schreckenbach, G.; Ziegler, T. *J. Phys. Chem. A* **1997**, *101*, 3388−3399.

(8) van Lenthe, E.; Wormer, P. E. S.; van der Avoird, A. *J. Chem. Phys.* **1997**, *107*, 2488−2498.

(9) Baerends, E. J.; Autschbach, J. A.; Bérces, A.; Bo, C.; Boerrigter, P. M.; Cavallo, L.; Chong, D. P.; Deng, L.; Dickson, R. M.; Ellis, D. E.; Fan, L.; Fischer, T. H.; Fonseca Guerra, C.; van Gisbergen, S. J. A.; Groeneveld, J. A.; Gritsenko, O. V.; Grüning, M.; Harris, F. E.; van den Hoek, P.; Jacobsen, H.; van Kessel, G.; Kootstra, F.; van Lenthe, E.; Osinga, V. P.; Patchkovskii, S.; Philipsen, P. H. T.; Post, D.; Pye, C. C.; Ravenek, W.; Ros, P.; Schipper, P. R. T.; Schreckenbach, G.; Snijders, J. G.; Sola, M.; Swart, M.; Swerhone, D.; Te Velde, G.; Vernooijs, P.; Versluis, L.; Visser, O.; van Wezenbeek, E.; Wiesenekker, G.; Wolff, S. K.; Woo, T. K.; Ziegler, T. *ADF*, 2002.01 ed.; SCM: Amsterdam, 2002.

(10) Te Velde, G.; Bickelhaupt, F. M.; van Gisbergen, S. J. A.; Fonseca Guerra, C.; Baerends, E. J.; Snijders, J. G.; Ziegler, T. *J. Comput. Chem.* **2001**, 931−967.

(11) Fonseca Guerra, C.; Snijders, J. G.; Te Velde, G.; Baerends, E. J. *Theor. Chem. Acc.* **1998**, *99*, 391.

(12) Slater, J. C. *Phys. Rev.* **1930**, *36*, 57.

(13) van Lenthe, E.; Baerends, E. J.; Snijders, J. G. *J. Chem. Phys.* **1993**, *99*, 4597.

(14) van Lenthe, E.; Baerends, E. J.; Snijders, J. G. *J. Chem. Phys.* **1994**, *101*, 9783.

(15) van Lenthe, E.; Ehlers, A. E.; Baerends, E. J. *J. Chem. Phys.* **1999**, *110*, 8943.

(16) van Lenthe, E.; van Leeuwen, R.; Baerends, E. J.; Snijders, J. G. *Int. J. Quantum Chem.* **1996**, *57*, 281.

(17) van Lenthe, E.; Snijders, J. G.; Baerends, E. J. *J. Chem. Phys.* **1996**, *105*, 6505.

(18) van Lenthe, E.; van der Avoird, A.; Wormer, P. E. S. *J. Chem. Phys.* **1998**, *108*, 4783−4796.

(19) Larsen, S. C. *J. Phys. Chem. A* **2001**, *105*, 8333−8338.

(20) Carl, P. J.; Isley, S. L.; Larsen, S. C. *J. Phys. Chem. A* **2001**, *108*, 4563−4573.

(21) van Lenthe, E.; van der Avoird, A.; Hagen, W. R.; Reijerse, E. J. *J. Phys. Chem. A* **2000**, *104*, 2070−2077.

(22) Stein, M.; van Lenthe, E.; Baerends, E. J.; Lubitz, W. *J. Phys. Chem. A* **2001**, *105*, 416−425.

(23) Boys, S. F. *Proc. R. Soc. (London) A* **1950**, *200*, 542.

(24) Arbuznikov, A. V.; Kaupp, M.; Malkin, V.; Reviakine, R.; Malkina, O. L. *Phys. Chem. Chem. Phys.* **2002**, *4*, 5467−5474.

(25) Munzarová, M. L.; Kaupp, M. *J. Phys. Chem. B.* **2001**, *105*, 12644−12652.

(26) Munzarová, M.; Kaupp, M. *J. Phys. Chem. A* **1999**, *103*, 9966−9983.

(27) Munzarová, M. L.; Kubacek, P.; Kaupp, M. *J. Am. Chem. Soc.* **2000**, *122*, 11900−11913.

(28) Barone, V. *J. Chem. Phys* **1994**, *101*, 6834.

(29) Barone, V. *Chem. Phys. Lett.* **1994**, *226*, 392.

(30) Abragam, A.; Bleaney, B. *Electron Paramagnetic Resonance of Transition Ions*; Clarendon Press: Oxford, U.K., 1970.

(31) Weil, J. A.; Bolton, J. R.; Wertz, J. E. *Electron Paramagnetic Resonance: Elementary Theory and Practical Applications*; John Wiley & Sons, Inc.: New York, 1994.

(32) Mahmoudkhani, A. H.; Casari, B.; Langer, V. *Z. Kristallogr.: New Cryst. Struct.* **2001**, *216*, 205−206.

(33) Pajunen, A.; Pajunun, S. *Acta Crystallogr.* **1980**, *B36*, 2425−2428.

(34) Oughtred, R. E.; Raper, E. S.; Shearer, H. M. M. *Acta Crystallogr.* **1976**, *B32*, 82−87.

(35) Frisch, M. J.; Trucks, G. W.; Schlegel, H. B.; Scuseria, G. E.; Robb, M. A.; Cheeseman, J. R.; Zakrzewski, V. G.; Montgomery, J. A., Jr.; Stratmann, R. E.; Burant, J. C.; Dapprich, S.; Millam, J. M.; Daniels, A. D.; Kudin, K. N.; Strain, M. C.; Farkas, O.; Tomasi, J.; Barone, V.; Cossi, M.; Cammi, R.; Mennucci, B.; Pomelli, C.; Adamo, C.; Clifford, S.; Ochterski, J.; Petersson, G. A.; Ayala, P. Y.; Cui, Q.; Morokuma, K.; Malick, D. K.; Rabuck, A. D.; Raghavachari, K.; Foresman, J. B.; Cioslowski, J.; Ortiz, J. V.; Stefanov, B. B.; Liu, G.; Liashenko, A.; Piskorz, P.; Komaromi, I.; Gomperts, R.; Martin, R. L.; Fox, D. J.; Keith, T.; Al-Laham, M. A.; Peng, C. Y.; Nanayakkara, A.; Gonzalez, C.; Challacombe, M.; Gill, P. M. W.; Johnson, B. G.; Chen, W.; Wong, M. W.; Andres, J. L.; Head-Gordon, M.; Replogle, E. S.; Pople, J. A. *Gaussian 98* (Revision A.6); Gaussian, Inc.: Pittsburgh, PA, 1998.

(36) Schafer, A.; Horn, H.; Ahlrichs, R. *J. Chem. Phys.* **1992**, *97*, 2571−2577.

(37) Schafer, A.; Huber, C.; Ahlrichs, R. *J. Chem. Phys.* **1994**, *100*, 5829−5835.

(38) Becke, A. D. *J. Chem. Phys.* **1993**, *98*, 5648−5652.

(39) Perdew, J. P.; Chevary, J. A.; Vosko, S. H.; Jackson, K. A.; Pederson, M. R.; Singh, D. J.; Fiolhais, C. *Phys. Rev. B* **1993**, *48*, 4978.

(40) Perdew, J. P.; Chevary, J. A.; Vosko, S. H.; Jackson, K. A.; Pederson, M. R.; Singh, D. J.; Fiolhais, C. *Phys. Rev. B* **1992**, *46*, 6671−6687.

(41) Becke, A. D. *Phys. Rev. A* **1988**, 3098−3100.
(42) Lee, C.; Yang, W.; Parr, R. G. *Phys. Rev. B* **1988**, *37*, 785−789.
(43) Miehlich, B.; Savin, A.; Stoll, H.; Preuss, H. *Chem. Phys. Lett.* **1989**, *157*, 200−206.
(44) Vosko, S. H.; Wilk, L.; Nusair, M. *Can. J. Phys.* **1980**, *58*, 1200.
(45) Perdew, J. P. *Phys. Rev. B* **1986**, *33*, 8822−8824.
(46) Perdew, J. P.; Burke, K.; Wang, Y. *Phys. Rev. B* **1996**, *54*, 16533−16539.
(47) Baerends, E. J.; Ellis, D. E.; Ros, P. *Chem. Phys* **1973**, *2*, 41−51.
(48) Versluis, L.; Ziegler, T. *J. Chem. Phys.* **1988**, *88*, 322−328.
(49) Te Velde, G.; Baerends, E. J. *J. Comput. Phys.* **1992**, *99*, 84−98.
(50) Guerra, C. F.; Snijders, J. G.; Te Velde, G.; Baerends, E. J. *Theor. Chem. Acc.* **1998**, *99*, 391−403.
(51) Frisch, A.; Frisch, M. J. *Gaussian 98 User's Reference*; Gaussian Inc.: Pittsburgh, PA, 1998; Vol. 6.0.
(52) Campbell, R. F.; Freed, J. H. *J. Phys. Chem.* **1980**, *84*, 2668−2680.
(53) Albanese, N. F.; Chasteen, N. D. *J. Phys. Chem.* **1978**, *82*, 910−914.
(54) Holyk, N. H. An EPR Study of Model Oxovanadium(IV) Complexes in Aqueous Solutions. M.S. Thesis, University of New Hampshire, 1979.
(55) Belanzoni, P.; Baerends, E. J.; van Asselt, S.; Langewen, P. *J. Phys. Chem.* **1995**, *99*, 13094−13102.
(56) Neese, F. *J. Chem. Phys.* **2001**, *115*, 11080−11096.
(57) Kaupp, M.; Reviakine, R.; Malkina, O. L.; Arbuznikov, A.; Schimmelpfennig, B.; Malkin, V. G. *J. Comput. Chem.* **2002**, *23*, 794−803.
(58) Saladino, A. C.; Larsen, S. C. *J. Phys. Chem. A* **2002**, *106*, 10444−10451.